

Experimental study of pharmacokinetics and radioimmunoimaging of ¹³¹Iodine-labeled monoclonal antibody E-B5 against Pro-Gastrin-Releasing Peptide(31-98)

Zeng-li LIU¹, Xiao-lin ZHOU²(Corresponding author), Li-Ye Liu¹, Yi-zhen SHI¹, Shou-ying DU⁴, Qiao-ling Xu³, Yong-mei SHEN¹, Yi YANG¹, Jun TANG¹

1 Department of Nuclear Medicine, The Second Affiliated Hospital of Soochow University, 1055 Sanxiang road, Suzhou, Jiangsu Province, China215004.

2 Department of Radiology and Nuclear Medicine, Chinese Institute for Radiation Protection, 102 Xuefu street, Taiyuan, Shanxi Province, China030006. **Corresponding author**

3 Department of Nuclear Medicine, the Fourth Hospital of Wuxi, Wuxi, Jiangsu Province, China214062.

4 Department of Pathology, University of California at San Diego Medical Center, USA

Abstract. Purpose: To investigate the radiolabeling of E-B5, a monoclonal antibody against Pro-Gastrin-Releasing Peptide(31-98) by ¹³¹Iodine and study the stability and immunoreactivity of ¹³¹I-E-B5. To determine the in vivo biodistribution of ¹³¹I-E-B5 in normal Kunming mouse and small cell lung cancer-bearing nude mouse models (SCLC mouse model) to study the pharmacokinetics of the ¹³¹I-E-B5 in vivo. Characterize the radioimmunoimaging effect and the best imaging time of ¹³¹I-E-B5 in different types of tumors. **Methods:** ¹³¹I-E-B5 was labeled by chloramine-T method. The labeling efficiency and radiochemical purity were determined by thin-layer chromatography. The ¹³¹I-E-B5 was incubated at 37°C water bath by itself or mixed with normal human serum, the radiochemical purity was then checked at different time points to determine its stability, and the immunoreactivity was determined by cell binding assays. ¹³¹I-E-B5 was injected into the tail veins of the normal Kunming mice which were sacrificed at different time points after injection, and the blood and representative tissues were collected immediately, and the %ID/g (percentage injected dose per gram of tissue) and pharmacokinetic parameters were calculated at various time points. Similarly, T/NT (tumor to non-tumor radioactivity ratio) at various time points were calculated after injection of ¹³¹I-E-B5 into the SCLC model. Mouse models bearing small cell lung cancer, lung adenocarcinoma, colon cancer were utilized to study the radioimmunoimaging effect of ¹³¹I-E-B5, and calculate the T/B ratio (tumor volume to the corresponding location at the other side). **Results:** ¹³¹I-E-B5 labeling rate was 90.8%, radiochemical purity was 99.28%, and radioactivity was 2.69 MBq/ug. The radiochemical purity of ¹³¹I-E-B5 was 90% after 6 hr at 37°C water bath, and remained at more than 70% after 24 hrs. The radiochemical purity was over 68.1% after 24 hrs mixing with normal human serum. The immunobinding rate of ¹³¹I-E-B5 to NCI-H446 (SCLC cell lines) and A549 (lung adenocarcinoma cell lines) was 71.6%, and 33.2%, respectively. The pharmacokinetics of ¹³¹I-E-B5 is consistent with a two-compartment model with first-order absorption. It was primarily metabolized via liver and kidney. The serum clearance rate is relatively fast. The %ID/g of ¹³¹I-E-B5 in xenografts was dramatically increased to a level much higher than other tissues 48 hrs after injection, reached plateau at 72 hr, and the T/NT ratio was also gradually increased with time. Prominent uptake of ¹³¹I-E-B5 in xenografts of SCLC in nude mice was observed after 24 hrs of injection. The radioactivity in the xenografts was gradually increased with time, and reached the peak at 72 and 96 hr. Xenografts of colon cancer showed similar results as that of SCLC although at a lower level. No observable accumulation was seen in the xenografts of lung adenocarcinoma. The T/B ratio in xenografts of SCLC was consistently higher than in colon cancer at all the time points, and both were significantly higher than that of lung adenocarcinoma which remained stable during the observation duration. **Conclusion:** The labeling rate and radiochemical purity of ¹³¹I-E-B5 were high and stable both in vivo and vitro. The labeled E-B5 kept its immunologic activity. ¹³¹I-E-B5 selectively accumulated at tumors expressing proGRP, and could effectively target SCLC, therefore is a promising radioimmunoimaging reagent for SCLC.

Keywords: Monoclonal antibody against pro-gastrin-releasing peptide(31-98) - ¹³¹I-E-B5 - Small cell lung cancer - Radioimmunoimaging

Introduction

The incidence and mortality rates of lung cancer are greatly increased in recent years. Lung cancer has become the number one killer in Chinese city-dwellers. Approximately 20-25% of lung cancers are categorized as small cell lung cancer (SCLC) which is fast growing, very aggressive, and with early distant

metastasis. SCLC is the most malignant lung cancer, and is usually at the late stage when a definitive clinical diagnosis is made. SCLC is treated very differently from non-small cell lung cancer (NSCLC), making a definitive diagnosis of pathological subtypes is an absolute requirement. Radioimmunoimaging and radioimmune targeted therapy have the advantages of high specificity, good targeting capability, and low toxicity. Developing a new generation of antibodies with optimal pharmacodynamics in vivo will benefit the early diagnosis and effective treatment for SCLC.

A peptide resembling bombesin at the carboxy-terminus was isolated from the porcine stomach, which comprises of 27-amino-acids, and functions as a stimulant of gastrin, therefore it is named gastrin releasing peptide (GRP)[1-2]. However, it is now known to perform many other functions including stimulation of the secretion of a variety of gastrointestinal hormones and pancreatic enzymes, and control of intestinal transit, metabolism and behavior[3-4]. GRP was also found to be expressed in the lungs of fetus and newborns, and the primary lung cancer especially SCLC[5]. It was discovered that SCLC could stimulate the secretion of GRP, and also has the GRP-receptors, indicating the presence of a self-regulatory circuit which could promote cell proliferation and the unlimited growth of tumor[6]. GRP was originally demonstrated by Maruno et al[7] in 1989 to be an important product of SCLC, and also to be an important tumor marker, and 72% of SCLC patients have increased serum GRP. Recent research demonstrates[8] that GRP was an auto-stimulatory growth factor of SCLC cells, and could promote rapid growth of tumor cells. However, clinical application is limited due to the instability of serum GRP and the difficulty in extracting GRP from the serum due to its very short half life[9].

ProGRP is the precursor of neuropeptide GRP, and has demonstrated good clinical performance in lung carcinoma patients for discriminating between NSCLC and SCLC and for classification of tumor subtypes[10]. There are three types of ProGRP which shares a common region (amino acids 31-98, ProGRP₍₃₁₋₉₈₎). Serum ProGRP level is stable and parallels the expression of GRP at gene and protein level. As a new SCLC tumor marker, research on ProGRP is very active[11-18]. A common method of preparing ProGRP₍₃₁₋₉₈₎[8,19,20] was to insert chemically synthesized cDNA into the EcoRI and SalI site of the expression vector pATTrp, recombinant human ProGRP₍₃₁₋₉₈₎ was expressed as a fusion protein with an amino-terminal 17-amino-acid sequence of TrpE protein in E.coli, followed by isolation and purification. Then, the extra amino acids were removed by cyanogen bromide, an extra step detrimental to production in large quantity which was further limited by subsequent isolation and purification.

More recently, genes encoding for ProGRP₍₃₁₋₉₈₎ were synthesized and inserted into the NheI and HindIII sites of expression vector pRSETc which has a strong promoter (Chinese Institute for Radiation Protection, Taiyuan, China). The human recombinant ProGRP₍₃₁₋₉₈₎ was expressed in BL₂₁DE₃, followed by isolation, purification and confirmation. The recombinant ProGRP₍₃₁₋₉₈₎ was used as an antigen to immunize Balb/c mouse, and a monoclonal antibody E-B5 subtyping as IgG2b subtype was successfully prepared. In this study, we labeled the E-B5 antibody using ¹³¹Iodine and established a small-cell lung cancer nude mouse model by xenografting NCI-H446, a SCLC cell line. The pharmacokinetics of ¹³¹I-E-B5 in vivo and the specificity of ¹³¹I-E-B5 in detecting SCLC were investigated via radioimmunoimaging study, in order to provide a specific and effective way to diagnose and treat SCLC.

Material and methods

Labeling, isolation and purification of ¹³¹I-E-B5. E-B5 (Chinese Institute for Radiation Protection) was labeled using ¹³¹Iodine via Aminochloride-T(Sigma-Aldrich, USA) method. The labeling rate was determined by thin-layer chromatography using Xinhua #1 filter paper as support, and natural saline as the solute. The R_f of ¹³¹I-E-B5 equals to 1/10, and that of ¹³¹I equals to 1.

The labeling liquid was loaded onto Sephadex G50 column (Amersham Pharmacia Biotech, USA), and the column was washed with 0.05 mol/L pH 7.5 PBS. The washing solution was subsequently collected into the centrifuge tubes in a volume of 5X10⁻⁴ L, and radioactivity was determined by a gamma counter (Capintec, Inc., USA). The first peak would be ¹³¹I-E-B5, and the second peak would be free ¹³¹Iodine. The radiochemical purity and radioactivity were determined by thin-layer chromatography.

Stability and immunoreactivity of ¹³¹I-E-B5. ¹³¹I-E-B5 was incubated in 37°C water bath for 2, 4, 6, 10, 12, and 24 hr in the presence or absence of human mixed serum from 10 persons respectively, and the radiochemical purity was further determined.

The immunoreactivity of ^{131}I -E-B5 was determined by cell binding assays [20]. The immunobinding rate is $B/T \times 100\%$, where T is the total radioactivity count per tube, and B is the radioactivity count of precipitated cells per tube.

In vivo biodistribution of ^{131}I -E-B5 in Kunming mouse. 30 normal healthy Kunming mice (Experimental Animal Center, Soochow University, Suzhou, China), half males and half females, with a body weight about 30 grams, were divided into 10 groups randomly. 1×10^{-4} L (1.48×10^{-1} MBq) of ^{131}I -E-B5 were injected into each mouse via tail vein, and all groups were sacrificed at 5 min, 15 min, 30 min, 1 hr, 2 hr, 4 hr, 8 hr, 12 hr, 24 hr, and 48 hr after injection. Blood, heart, spleen, lung, kidney, small intestine, skeletal muscle, and brain were collected, weighed, and the radioactivity counts (cpm) was determined. Finally, the %ID/g was calculated. The pharmacodynamics of the ^{131}I -E-B5 was further calculated by %ID/g at different points using the Microcal Origin⁷ software.

Establishment of nude mouse model. SCLC cell line NCI-H446 (lab stock) was maintained regularly. Cells at log phase were collected and prepared at a concentration of 2×10^7 /mL in DMEM. 0.2 mL was injected subcutaneously into the right upper arm of each BALB/c-neu nud mouse (Shanghai Experimental Animal Center, Shanghai, China), which were 3-4 weeks old, half males and half females, at the average body weight of 20 grams. The recipient mice were kept in sterile incubator, and were observed regularly for general condition, food intake and tumor growth. The mice were used for further studies when the xenograft grows up to $1.5 \times 1.5 \times 1.0$ cm³.

A549 lung adenocarcinoma, and LOVL colon cancer xenograft models were similarly established in BALB/c-neu nude mouse.

In vivo biodistribution of ^{131}I -E-B5 in nude mouse model with SCLC xenograft. 18 nude mice with SCLC xenograft were randomly divided into 6 groups and were each injected 0.1 mL of ^{131}I -E-B5 (0.148 MBq) via tail vein. The mice were sacrificed at 1, 2, 24, 48, 72, and 96 hr respectively, and blood, heart, spleen, lung, kidney, small intestine, skeletal muscle, brain and tumor were collected, weighed, and the radioactivity counts (cpm) was determined. Finally, the %ID/g was calculated for each time point. The radioactivity count ratio of Tumor/Non-Tumor tissue at each time point was also determined.

Radioimmunoimaging study. 3 nude mice from each group of SCLC, lung adenocarcinoma, and colon cancer models were fed with 0.1% KI in 5% glucose solution 3 days before the imaging study to saturate the thyroid. The mice were fixed in a prone position, and 0.2 mL of ^{131}I -E-B5 (7.4 MBq) was injected into each mouse via tail vein, and the still images were taken at 1, 4, 8, 12, 24, 48, 72, and 96 hr respectively, using the Axis Dual Head SPECT (Philips Healthcare, Netherlands). The data was collected at a preset 1000 kcts, at a magnification of 1.6 and a matrix of 64×64 . The ratio of tumor to the contralateral corresponding normal tissue (T/B ratio) was then calculated by ROI technique.

Statistical analysis. The Student's t-test was used to determine the statistical significance between two groups.

Results

Labeling, isolation and purification of ^{131}I -E-B5

The elution dynamics after loading the labeling liquid on Sphaex G50 was as illustrated in Figure 1. The labeling rate of ^{131}I -E-B5 is 90.8%, the radiochemical purity is 99.28%, and the radioactivity is 2.69 MBq/ug. The radiochemical purity of ^{131}I -E-B5 is still over 70% after incubation at 37°C for 24 hr, which is approximately 68.1% if mixed thoroughly with normal human serum. The immunoreactivity of E-B5 is relatively good after labeling. The immunobinding ratio of ^{131}I -E-B5 in H446 and A549 cell lines is 71.6%, and 33.2% respectively, which is of statistical significance ($P < 0.05$).

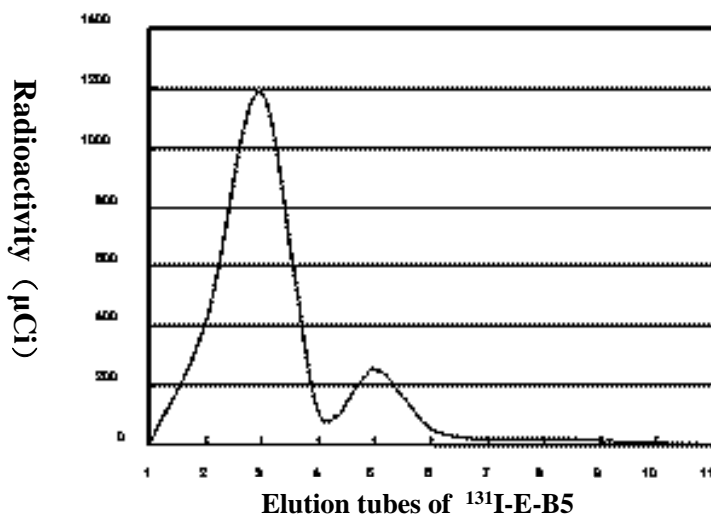


Figure 1. Elution curve of $^{131}\text{I-E-B5}$

In vivo biodistribution of $^{131}\text{I-E-B5}$ in Kunming mouse

The %ID/g for various organs at different time points were summarized in Table 1. $^{131}\text{I-E-B5}$ was distributed mostly in the liver, lung, kidney, but not in intestine, skeletal muscle and brain. The metabolism of $^{131}\text{I-E-B5}$ in healthy Kunming mouse is consistent with a two-compartment model with first-order absorption. The metabolism formula $c = 0.08e^{0.083} + 0.59e^{3.125}$ was calculated through regression analysis. The half-life of fast-phase and slow-phase clearance is 0.2 hr ($T_{1/2\alpha}$), and 8.35 hr ($T_{1/2\beta}$), respectively.

Table 1. %ID/g (percentage injected dose per gram of tissue) for various organs in Kunming mouse

Organs	Time points after injection of $^{131}\text{I-E-B5}$									
	5 min	15 min	30 min	1 hr	2 hr	4 hr	8 hr	12 hr	24 hr	48 hr
Heart	0.14±0.01	0.11±0.02	0.08±0.01	0.07±0.01	0.09±0.02	0.08±0.02	0.08±0.01	0.07±0.00	0.04±0.01	0.03±0.01
Liver	0.26±0.01	0.24±0.08	0.19±0.04	0.11±0.02	0.10±0.01	0.09±0.02	0.07±0.00	0.08±0.01	0.07±0.01	0.03±0.01
Spleen	0.19±0.04	0.14±0.02	0.15±0.03	0.11±0.02	0.10±0.01	0.07±0.02	0.09±0.05	0.08±0.00	0.06±0.01	0.03±0.01
Lung	0.28±0.12	0.26±0.08	0.22±0.03	0.12±0.06	0.10±0.03	0.09±0.05	0.09±0.17	0.06±0.02	0.06±0.02	0.03±0.01
Kidney	0.26±0.02	0.24±0.02	0.21±0.02	0.15±0.02	0.13±0.02	0.13±0.00	0.11±0.05	0.09±0.01	0.08±0.01	0.06±0.01
Stomach	0.11±0.03	0.10±0.03	0.09±0.02	0.08±0.00	0.12±0.03	0.09±0.01	0.10±0.07	0.10±0.03	0.07±0.02	0.05±0.01
Intestine	0.09±0.02	0.07±0.02	0.08±0.01	0.07±0.02	0.10±0.01	0.08±0.01	0.09±0.01	0.05±0.01	0.04±0.01	0.03±0.00
Skeletal	0.14±0.02	0.13±0.02	0.11±0.04	0.12±0.03	0.10±0.01	0.09±0.02	0.08±0.11	0.07±0.02	0.09±0.14	0.05±0.02
Muscle	0.07±0.02	0.05±0.01	0.03±0.00	0.04±0.00	0.03±0.01	0.03±0.01	0.01±0.00	0.03±0.00	0.02±0.00	0.02±0.01
Brain	0.06±0.01	0.04±0.00	0.04±0.01	0.03±0.00	0.03±0.01	0.03±0.00	0.05±0.00	0.03±0.00	0.02±0.01	0.01±0.00
Blood	0.74±0.03	0.61±0.10	0.39±0.17	0.35±0.02	0.29±0.07	0.27±0.07	0.25±0.03	0.23±0.27	0.20±0.02	0.12±0.03

In vivo biodistribution of $^{131}\text{I-E-B5}$ in nude mouse model with SCLC xenograft

At 48 hr after injection of $^{131}\text{I-E-B5}$, the %ID/g of tumor mass was much higher than that of other organs/tissues which reached the peak level at 72 hr (Table 2). The T/NT of tumor to other organs/tissues gradually increases with time, and the T/NT is over 1.0 at 48 hr for most organs/tissues except blood (Table 3).

Table 2. %ID/g (percentage injected dose per gram of tissue) for various organs at various time points after injection of $^{131}\text{I-E-B5}$ in nude mouse model with SCLC xenograft

Organs	Time points after injection of ¹³¹ I-E-B5					
	1 hr	12 hr	24 hr	48 hr	72 hr	96 hr
Heart	0.10±0.02	0.06±0.01	0.06±0.01	0.05±0.01	0.03±0.01	0.03±0.00
Liver	0.17±0.05	0.13±0.01	0.10±0.05	0.08±0.04	0.04±0.00	0.04±0.00
Spleen	0.17±0.06	0.08±0.01	0.12±0.05	0.08±0.02	0.06±0.20	0.05±0.01
Lung	0.14±0.04	0.09±0.15	0.08±0.04	0.06±0.21	0.05±0.03	0.03±0.15
Kidney	0.14±0.04	0.07±0.01	0.06±0.30	0.05±0.01	0.04±0.01	0.03±0.00
Stomach	0.06±0.01	0.04±0.01	0.04±0.02	0.04±0.01	0.02±0.01	0.03±0.01
Intestine	0.09±0.02	0.06±0.01	0.08±0.01	0.06±0.01	0.04±0.00	0.03±0.00
Brain	0.03±0.01	0.02±0.01	0.02±0.01	0.02±0.01	0.02±0.04	0.02±0.01
Skeletal	0.23±0.08	0.19±0.01	0.12±0.01	0.10±0.18	0.07±0.02	0.06±0.01
Muscle	0.04±0.01	0.06±0.04	0.05±0.01	0.03±0.01	0.03±0.01	0.03±0.01
Tumor	0.04±0.01	0.06±0.01	0.06±0.11	0.10±0.01	0.14±0.03*	0.10±0.01
Blood	0.73±0.30	0.23±0.03	0.25±0.07	0.14±0.04	0.08±0.01	0.09±0.01

*:compared with other organs, p<0.01

Table 3. T/NT (tumor to non-tumor radioactivity ratio) at various time points after injection of ¹³¹I-E-B5 in nude mouse model with SCLC xenograft

Organs	Time points after injection of ¹³¹ I-E-B5					
	1 hr	12 hr	24 hr	48 hr	72 hr	96 hr
Tumor/ Heart	0.42±0.02	1.06±0.01	1.11±0.01	2.04±0.01*	4.67±0.01 **	3.33±0.21
Tumor/Liver	0.24±0.05	0.46±0.03	0.62±0.05	1.25±0.04*	3.50±0.06**	2.52±0.13
Tumor/Spleen	0.24±0.06	0.75±0.01	0.51±0.05	1.25±0.02*	2.33±0.03**	2.32±0.06
Tumor/Lung	0.29±0.04	0.67±0.15	0.75±0.04	1.67±0.21*	2.83±0.12**	3.35±0.54
Tumor/Kidney	0.29±0.04	0.85±0.04	1.06±0.30	2.32±0.01*	3.55±0.21**	3.23±0.41
Tumor/Stomach	0.67±0.01	1.52±0.01	1.50±0.32	2.51±0.01*	7.01±0.52**	3.42±0.65
Tumor/Intestine	0.44±0.02	1.12±0.05	0.75±0.01	1.67±0.03*	3.52±0.56**	3.33±0.02
Tumor/Brain	1.33±0.01	3.31±0.01	3.33±0.21	5.03±0.18*	7.02±0.68**	5.03±0.54
Tumor/Skeletal	0.17±0.01	0.32±0.01	0.54±0.01	1.21±0.02*	2.03±0.23**	1.66±0.22
Tumor/Muscle	1.02±0.01	1.20±0.04	1.23±0.02	3.33±0.08*	4.67±0.66**	3.33±0.85
Tumor/Blood	0.05±0.03	0.26±0.03	0.24±0.07	0.71±0.06*	1.75±0.64**	1.11±0.78

*:compared with 1hr,12 hr and 24 hr, p<0.01; **:compared with 48hr, p<0.01.

Radioimmunoimaging study

As demonstrated in Figure 2, at 1 hr after injection of ¹³¹I-E-B5, the tumor mass in nude mouse model with SCLC xenograft started to show up on the imaging study. With time, the radioactivity uptake gradually increased at the tumor site and the contrast with nearby normal tissue also gradually elevated. At 24 hr, the tumor mass was apparent on imaging, and reached the best resolution at 72 and 96 hr. This observation was consistent with the *in vivo* biodistribution of ¹³¹I-E-B5 in nude mouse model with SCLC xenograft.

Similarly, the imaging result of colon cancer mouse model is comparable to that of SCLC model although with much less contrast between the tumor and contralateral normal tissue (Figure 3).

Not surprisingly, no apparent accumulation of radioisotope in the tumor mass in lung adenocarcinoma mouse model from 1 to 96 hr after injection of ¹³¹I-E-B5 (Figure 4).

The T/B ratios of tumor mass to the corresponding contralateral site at the various time points were summarized in Table 4. The T/B ratios of SCLS and colon cancer xenografts progressively increased with time, while that of lung adenocarcinoma remained unchanged. The T/B ratios of SCLS and colon cancer xenografts were much higher than that of lung adenocarcinoma xenograft from 24 hr after injection ($P<0.05$), with the ratio of SCLC higher than that of colon cancer ($P<0.05$).

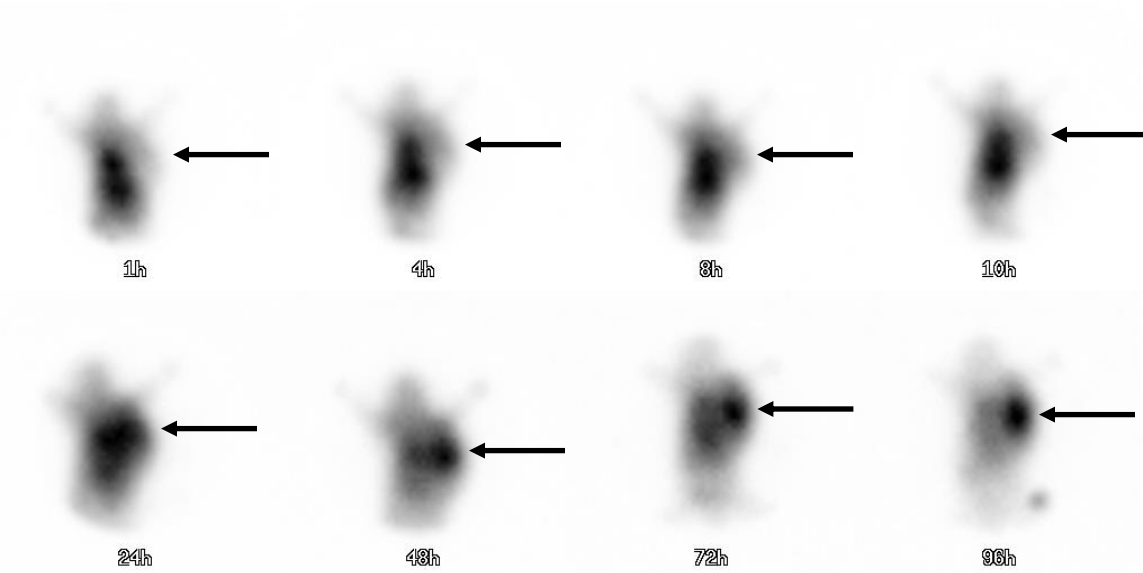


Figure 2. Radioimmunoimaging with ^{131}I -E-B5 in SCLC mouse model (arrows demonstrated to the location of tumor mass)

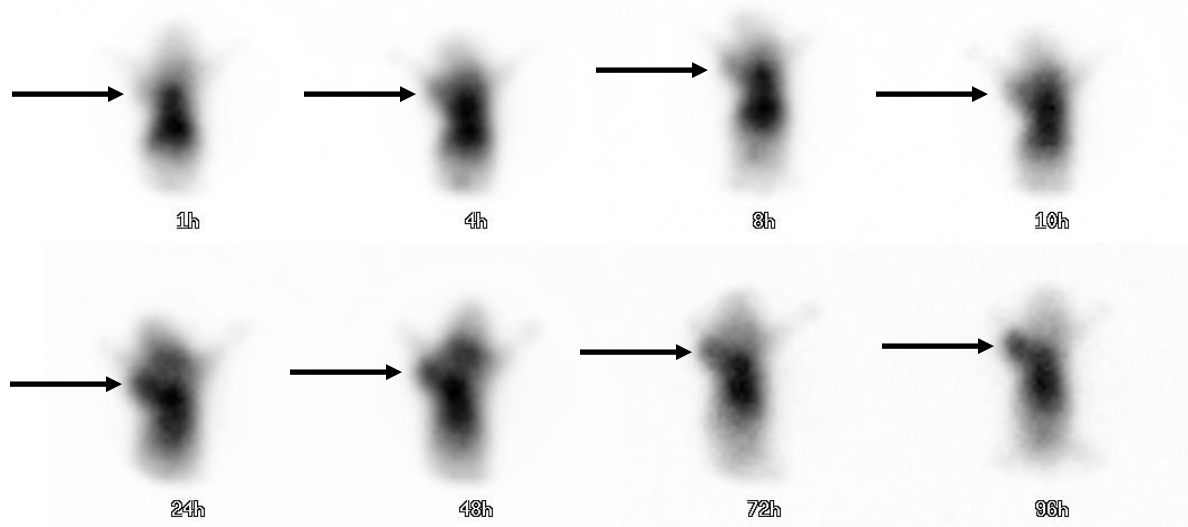


Figure 3. Radioimmunoimaging with ^{131}I -E-B5 in colon cancer mouse model. (arrows demonstrated to the location of tumor mass)

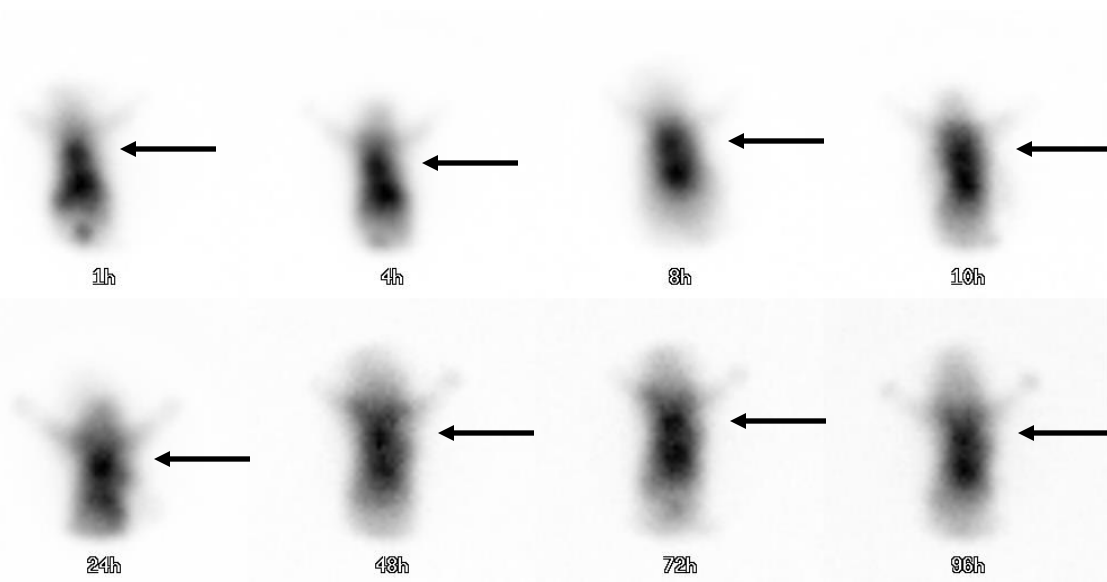


Figure 4. Radioimmunoimaging with ^{131}I -E-B5 in lung adenocarcinoma mouse model (arrows demonstrated to the location of tumor mass)

Table 3. T/B ratio (tumor volume to the corresponding location at the other side) at the various time points after injection of ^{131}I -E-B5 in nude mouse model with various tumor xenografts

Types of xenograft	Time points after injection of ^{131}I -E-B5							
	1 hr	4 hr	8 hr	10 hr	24 hr	48 hr	72 hr	96 hr
SCLC	1.27±0.57	1.36±0.55	1.49±0.65	1.63±0.49	3.31±0.28*	3.98±0.55*	5.27±0.97*	5.82±0.89*
colon cancer	1.15±0.32	1.24±0.45	1.35±0.68	1.42±0.33	1.55±0.73Δ	1.67±0.38Δ	2.28±0.72Δ	2.57±0.58Δ
lung adenocarcinoma	1.30±0.37	1.29±0.53	1.31±0.56	1.25±0.71	1.24±0.69	1.27±0.59	1.26±0.65	1.29±0.87

*:at the same time point, compared with the group of colon cancer and lung adenocarcinoma , $p<0.01$;
 at the same time point,compared with the group of lung adenocarcinoma , $p<0.05$;

Discussion

The common methods of labeling antibodies include Aminochloride-T, Lipoperoxidase(LPO), and Iodogen iodination. Aminochloride-T is the most widely used method due to its high efficiency, good repetitivity, and low cost of reagents. We therefore used this method to label E-B5. The resulting ^{131}I -E-B5 has a labeling rate of 90.8%, and radiochemical purity of 99.28%. The radiochemical purity of the ^{131}I -E-B5, with and without mixing with normal human serum, is 68.1% and over 70% respectively, after 24 hr of incubation at 37°C water bath. The immuno-binding rate of ^{131}I -E-B5 to NCI-H446 SCLC cell line is 71.6%, indicating that ^{131}I -E-B5 is stable and with good immunoreactivity.

The pharmacodynamics of ^{131}I -E-B5 in normal Kunming mouse is consistent with a two-compartment model with first-order absorption. The half life of fast-phase and slow-phase clearance is 0.2 hr ($T_{1/2\alpha}$), and 8.35 hr ($T_{1/2\beta}$) respectively. ^{131}I -E-B5 is distributed in all the tested tissues. Initially, i.e. 5 min after

injection, ¹³¹I-E-B5 is mostly distributed in the liver, lung, and kidney. The ID%/g of the above three organs is gradually reduced with time. The quickest reduction occurred in the first 60 min, with the ID%/g of the liver, lung, and kidney dropped to 42.3%, 42.9% and 57.7% of the original level respectively. Then, the reduction speed is slowed down and is maintained at a low level. The serum radioactivity is the highest, followed by kidney which is significantly higher than intestine and is still higher than all the organs/tissues tested except serum 1 hr after injection. The radioactivity in intestine, skeletal muscle, and brain is maintained at very low level through the whole study time. This indicates that the monoclonal antibody is mostly metabolized in liver and kidney, with a quick clearance from the serum, a low uptake by organs/tissues like the intestine and skeletal muscle. These properties are beneficial to radioimmunological imaging study and other related research for diagnosis and treatment of diseases.

The in vivo biodistribution study of ¹³¹I-E-B5 in SCLC nude mouse model demonstrated that the %ID/g of tumor and the T/NT of tumor to various organs/tissues increased with the incubation time. At 48 hr, the %ID/g of tumor was much higher than other organs/tissues, and the T/NT of tumor to various organs/tissues is more than 1.0 except serum. At 72hr, the %ID/g of tumor and the T/NT of tumor to various organs reached their peak level, with the T/NT of tumor to various organs/tissues over 2.0 (except serum), and the T/NT of tumor to muscle was as high as 4.67. Although this ratio was slightly reduced after 72 hr, the reduction was not statistically significant ($P>0.05$). Possible reasons for the reduction of T/NT include: the available target antigen in the tumor is gradually reduced; the relative radioactivity accumulated in the tumor is reduced due to the physical and biological decay; the immunoreactivity of some ¹³¹I-E-B5 molecules is gradually reduced leading to the loss of its specific binding capability to tumor cells and subsequent clearance from serum.

As demonstrated in radioimmunoimaging (Figure 2), in 24 hr after injection into the SCLC nude mouse model via tail vein, the ¹³¹I-E-B5 mostly accumulated at the trunk including the chest and abdomen, with much less in the tumor. After 24 hr, apparent uptake by the tumor started to show up and steadily increased with longer incubation as reflected by the increased T/B ratio. At 72 and 96 hr, the T/B value reached its peak with the best imaging result. This is consistent with the in vivo biodistribution of ¹³¹I-E-B5 in SCLC mouse model. ProGRP is the precursor of GRP, and its level reflects the GRP level at both transcriptional and translational levels [8,9,19]. The GRP produced by SCLC is normally stored in the Golgi apparatus, and will be released into the tumor tissue and bind to the GRP receptor on the cell membrane thereby promoting the proliferation and unlimited growth of tumor cells [20-22]. ¹³¹I-E-B5 could bind directly with the GRP released into the extracellular space of the tumor tissue, or could possibly bind to the GRP in the Golgi apparatus by being uptaken into the cytoplasm after being degraded into small molecules by various enzymes. Accumulation of ¹³¹I-E-B5 in the tumor thereby creates a clear radioimage.

The ¹³¹I-E-B5 was not accumulated in the xenografted lung adenocarcinoma, which is consistent with the fact that the adenocarcinoma expresses only very low levels of GRP. These results indicate that ¹³¹I-E-B5 could potentially benefit the differential diagnosis of SCLC.

Of note, the GRP is also expressed in the gastrointestinal tumors. Studies in the colon cancer cell lines showed that they universally express GRP and GRP receptor mRNA which lead to the release of the intracellular Ca²⁺ but not the growth of tumor cells [6-7]. The radioimaging studies of colon cancer mouse model demonstrated that prominent accumulation of ¹³¹I-E-B5 in the xenograft did occur consistent with the expression of GRP in these cells.

Our study indicates that ¹³¹I-E-B5 could selectively accumulate in the tumor site of SCLC xenograft mouse model with strong contrast with the nearby normal tissues with the best imaging time being 72 and 96 hr. This will potentially provide an effective diagnostic tool for SCLC. However, the longer duration needed to obtain the best imaging result is a hinder to the potential clinical application. Smaller fragments of antibodies and labeling with radioisotope of shorter half-life such as ^{99m}Tc would be the focus of future research.

References

1. McDonald TJ, Nilsson G, Vagne M, et al. A gastrin releasing peptide from the porcine nonantral gastric tissue. *Gut* 1978; 19: 767-774.
2. McDonald TJ, Jornvall H, Nilsson G, et al. Characterization of a gastrin releasing peptide from porcine non-antral gastric tissue. *Biochem Biophys Res Commun* 1979; 90:227-233

3. Bunnett N. Gastrin releasing peptide. In: Walsh JH, Dockray GJ, editors. Gut peptides. New York: Raven Press, 1994. p.423-55.
4. Yamada K, Wada E, Wada K. Bombesin-like peptides: studies on food intake and social behaviour with receptor knock-out mice. *Ann Med* 2000; 32:519-529
5. McDonald TJ, Ghatei MA, Bloom SR, et al. A qualitative comparison of canine plasma gastroenteropancreatic hormone response to bombesin and the porcine gastrin-releasing peptide (GRP). *Regul Pept* 1981; 2(5):293-304.
6. Moody TW, Russell EK, O'Donohue TL, et al. Bombesin-like Peptides in small cell lung cancer :biochemical characterization and Secretion from a cell line. *Life Sci* 1983; 32(5):487-493.
7. Maruno K, Yamaguchi K, Abe K, et al. Immunoreactive gas-trin releasing peptide as a specific tumor marker in patients with small cell lung carcinoma. *Cancer Res* 1989; 49(3):629-632.
8. Uchida K, Kojima A, Morokawa N, et al. Expression of pro-gastrin releasing peptide and gastrin-releasing peptide receptor mRNA transcripts in tumor cells of patients with small cell lung Cancer. *J Cancer Res Clin Oncol* 2002; 128(12):633-640.
9. Miyake Y, Kodama T, Yamaguchi K. Progastrin-releasing peptide(31-98) is a specific tumor marker in patients with small cell lung carcinoma [J]. *Cancer Res* 1994; 54(8) ; 2136-2140.
10. Stieber P, Dienemann H, Schalhorn A, Schmitt UM, Reinmiedl J, Hofmann K, Yamaguchi K: Pro-gastrin-releasing peptide (ProGRP) – a useful marker in small cell lung carcinomas. *Anticancer Res* 1999; 19:2673-2678.
11. Winther B, Moi P, Paus E, et al. Targeted determination of the early stage SCLC specific biomarker pro-gastrin-releasing peptide (ProGRP) at clinical concentration levels in human serum using LC-MS. *J Sep Sci* 2007; 30(16):2638-2646.
12. Winther B, Paus E, Reubsaet JL. Determination of the small cell lung cancer associated biomarker pro-gastrin-releasing peptide (ProGRP) using LC-MS. *J Sep Sci* 2007; 30(2):234-240.
13. Yamaguchi H, Soda H, Kitazaki T, et al. Serum progastrin-releasing peptide levels followed by whole-body positron emission tomography detects early recurrence of small-cell lung cancer. *Respirology* 2007;12(1):137-139.
14. Satoh H, Kagohashi K, Kurishima K, et al. Comparison of neurone-specific enolase and pro-gastrin releasing peptide in the prognostic evaluation of small cell lung cancer patients. *Clin Oncol (R Coll Radiol)* 2006;18(9):720.
15. Matsubayashi H, Fujiwara S, Kobayashi Y, et al. A small cell carcinoma of the pancreas with a high level of serum ProGRP. *J Clin Gastroenterol* 2004; 38(9):834-835.
16. Molina R, Filella X, Auge JM. ProGRP: a new biomarker for small cell lung cancer. *Clin Biochem* 2004;37(7):505-511.
17. Oremek GM, Sapoutzis N. Pro-gastrin-releasing peptide (Pro-GRP), a tumor marker for small cell lung cancer. *Anticancer Res* 2003;23(2A):895-898.
18. Schneider J, Philipp M, Salewski L, et al. Pro-gastrin-releasing peptide (ProGRP) and neuron specific enolase (NSE) in therapy control of patients with small-cell lung cancer. *Clin Lab* 2003; 49(1-2):35-42.
19. Nordlund MS, Fermer C, Nilsson O. et al. Production and Characterization of Monoclonal Antibodies for Immunoassay of the Lung Cancer Marker proGRP. *Tumour Biol* 2007; 28(2):100-110.
20. Dumesny C, Patel O, Lachal S, et al. Synthesis, expression and biological activity of the prohormone for gastrin releasing peptide (ProGRP). *Endocrinology* 2006; 147(1):502-509.
21. O'Grady LF, DeNardo G, DeNardo S. Radiolabelled monoclonal antibodies for the detection of cancer. *Am J Physiol Imaging*. 1986;1(1):44-53
22. Zhou Ming-fei; Zhang He-qiu; Ling Shi-gan .Enzyme linked immunosorbent assay of pro gastrin releasing peptide as tumor marker for small cell lung carcinoma: research advances and clinical application. *Bulletin of the Academy of Military Medical Sciences* 2000; 24(2):143-146.